Proceedings of PVP2005
2005 ASME Pressure Vessels and Piping Division Conference
July 17-21, 2005, Denver, Colorado USA
PVP2005-71724

APPLICATIONS OF LIMIT LOAD ANALYSES TO ASSESS THE STRUCTURAL INTEGRITY OF PRESSURE VESSELS

Richard C. Biel, P.E.
Stress Engineering Services, Inc.
richard.biel@stress.com

Chris Alexander
Stress Engineering Services, Inc.
chris.alexander@stress.com

ABSTRACT

With advances in computational modeling techniques, limit load methods are gaining wider acceptance as a tool for determining the structural integrity of pressure vessels. The objective of a limit load analysis is to size a vessel or structure considering nonlinear methods such as elastic-plastic material properties and non-linear strain-displacement relations. Case studies are presented in this paper that feature external pressures, gravity, and wind loads. The technique applies an appropriate initial magnitude for each load type and uses the analysis model to increase the load until a lower bound is calculated. The lower bound value is determined by incrementally increasing the load until convergence is not possible then the results are extracted.

This paper presents how limit load techniques were used to address the structural integrity of four engineered systems including the structural stability of a corroded tower under wind and vacuum loads, determining the pressure capacity of a pressure vessel, analysis of a subsea vessel under high external pressures, and the remaining buckling resistance of a dented subsea flowline. The paper highlights the application of limit load techniques using criteria detailed in WRC 464.

ANALYSIS METHODS AND RESULTS

Limit load analysis methods are useful for addressing a range of structural geometries and loading types. The methods are relatively straight forward as demonstrated by the details provided in the following sections of this paper.

Corroded Tower

A chemical company was concerned whether a tower that had suffered some metal loss corrosion was able to withstand wind loads and external pressure loads with adequate margins. Finite element analyses were run for the tower as-inspected and with added reinforcement to determine limit loads and calculate Design Margins (DM) based on these limit loads.

The ASME Boiler & Pressure Vessel Code, Section VIII, Division 2 [1] describes an analysis-based approach and WRC Bulletin 464 [2] outlines specific procedures used to perform this study.

The following definition is helpful to understand the analysis methodology:

> *Limit Analysis – Limit analysis is a special case of plastic analysis in which the material is assumed to be ideally plastic (non-strain hardening). [In this work, limit analysis is used to compute the collpse load, known as the lower bound limit load, the load associated with a statically admissible field.]*

The tower is an insulated pressure vessel with many nozzles, trays, and external piping. It is about 11.15 feet (3505 mm) in diameter and 144.88 feet (44160 mm) in height including the support skirt and overhead nozzle. The tower shells were originally designed for full vacuum external pressure and a basic wind speed of 100 miles per hour (MPH) (161 kph). The upper half of the tower was made using 0.394-inch (10 mm) thick stainless steel, while the lower half including the skirt was made from 0.433-inch (11 mm) thick stainless steel material.

Two configurations were analyzed for gravity or self-weight, wind, and external pressure. The first was the corroded basic tower and second was the corroded tower with added longitudinal stiffeners. Both included tray support rings as they added some stiffness to the structure. Longitudinal stiffeners were added to the analysis model over the corroded area between elevations 5075 and 8450. Since the analysis model was not originally built for these stiffeners, they were added using contact surfaces with the properties that were the mathematical equivalent of welding them in place.

A three dimensional shell-element finite element analysis model was made using 1/2 symmetry by reference to the construction drawings and hand sketches for the longitudinal stiffeners to be added. The insulation, nozzles, and external piping were simulated by adding weight and an effective outside diameter that accounted for the wind overturning moment profile. External piping loads were not used.

Figure 1 shows the model that was used in the analysis. This figure shows the free “edges” of the model features so that the entire model can be visualized.

The shell thickness values of the tower model between two elevations were adjusted for corrosion. The corroded zones, 12 bands, were assigned the remaining thickness to be the mean of the data minus two standard deviations over the zone.

The ovality was specified to be 1 percent of the vessel diameter for all models used in the analyses with the ovality in the least favorable orientation relative to wind direction (i.e. minor diameter parallel to wind direction). The weight was checked during the “gravity” load step. This was considered important to fully account for the compressive loads and stresses in the area of interest. Material properties at 250ºF were used

throughout and assumed to be elastic, perfectly plastic with yield strength of 25.0 ksi. This is considered conservative since austenitic stainless steels exhibit significant strain hardening.

To determine the DMs with respect to wind load, a limit analysis was performed by ramping up the basic wind load to failure. The basic wind load was set by using the methods of ASCE-7 [3]. Since the wind load is non-linear with respect to wind velocity as well as elevation above grade, only the basic wind load was calculated and failure load was calculated as multiples of the basic wind load or DM. The wind is ramped up with a target of three times the basic load (3X). The analysis is stopped when the increment is reduced to a small value. The final calculated DM is the accumulated fraction of load times the target load.

To determine the DM with respect to external pressure, the material was assumed elastic-plastic with the yield stress set at the minimum specified material yield stress. The basic gravity and wind loads were first imposed, then the external pressure was ramped up to failure with a target of about four times the vacuum (4X). The analysis was stopped when convergence was no longer possible or the run was stopped by the analyst because the increment of additional load was not significant. The final calculated DM is the accumulated fraction of load multiplied by the target load. The DM is considered to be the margin of the calculated limit pressure over the vacuum pressure.

Analysis processing was done using the ABAQUS [4] general purpose finite element analysis software. For this problem, both non-linear elastic-plastic material properties and non-linear geometric properties were used. Loads that cause the stresses to exceed the yield strength were redistributed so as to keep the material along the stress-strain curve while accumulating plastic strain. The structure does not return to its original shape upon removal of forces. The non-linear geometry changed the shape of the cylinder into an oval that reduced stiffness with respect to resisting further deformations.

For the tower analyses, the first step was the imposition of gravity in every run. When solving for the wind load, the second step added the external pressure and the third step ramped up the wind load to failure. When solving for the external pressure load, the second step added the basic wind load and the third step ramped up the external pressure load to failure.

The ABAQUS viewer post-processor was used to extract nodal displacements and plot the color contour stress and displacement results. In these non-linear analyses, the precise values of stresses were not significant since the upper limit of stress was fixed as the value of yield strength.

The color contour plots of the results of the analyses were reduced to the minimum number needed to describe the behavior of the vessel under loading.

Figure 2 shows the stress results of adding gravity and external pressure to the model, followed by ramping up the wind load until the structure was unable to support additional load.

Figure 3 shows the results of the limit analysis on the entire structure. In this figure, the contour plots were minimum principal strain (compressive) showing the areas that were beginning to undergo plastic deformation.

Figure 4 shows the stress results of adding gravity and the basic wind load to the model, followed by ramping up the external pressure until the structure was unable to support additional external pressure.

In **Table 1**, the Analysis Limit was the step time or fraction of the target loading. The DM was calculated by multiplying the Analysis Limit and the target loading, either wind or external pressure as applicable.

The results of the analyses showed that the corroded tower was fit for continued service and that the gains from the additional longitudinal reinforcement were marginal.

Table 1: Analyses Cases and Results

Pressure psi/bar	Wind Load[1]	Reinforced[2]	Analysis Limit[3]	DM[4]	Ramp Load
-14.5/-1.0	3X	No	0.59	1.78	wind
0.0/0.0	3X	No	0.61	1.83	wind
-14.5/1.0	3X	Yes	0.79	2.36	wind
0	3X	Yes	0.82	2.46	wind
-58.8/4.0	1X	Yes	0.55	2.19	press
-58.8/4.0	1X	No	0.54	2.18	press

Notes:
1. Wind load is the multiple of the overturning load due to 100 MPH (161 KPH) wind.
2. Reinforced with longitudinal stiffeners.
3. Analysis limit is the fraction of the target ramp load that was achieved during the analysis.
4. The Design Margin is calculated as the margin against the limit load under the specified loading.

Pressure Vessel Overpressure Capacity

A chemical company was concerned that the capacity of a relief system was inadequate to prevent possible overpressure events. The concern was that excursions of internal pressure, above the original pressure rating of the equipment, might occur. The owner recognized that it was important to determine the maximum internal pressure that the vessels could withstand within recognized standards. Stress Engineering Services, Inc. was asked to perform an analysis of the primary pressure vessels. These vessels are made of carbon steel material originally designed using the ASME Code, Div. 1 but since the construction details corresponded to ASME Code, Div. 2, the latter was used in this assessment. WRC Bulletin 464 outlines procedures to be used.

The FEA mesh consisted chiefly of four-node, three-dimensional quadrilateral shell elements, S4R. A few triangular elements were used as necessary to complete the model transitions. Nozzle details were simplified by using increased shell thickness for the reinforcing pads. A node set was made by defining a centrally located node at the end of the each nozzle to track the nozzle displacements under load. **Figure 5** shows the model that was used in the analysis.

The vessels were built at different times and were similar but not identical. An exemplar vessel was used for the analysis that was a composite of all the vessels that included the most conservative design thickness values from the information provided. Each of the nozzles was covered with a domed head in order to develop the correct pressure end loads. External piping loads were not included in this analysis.

Most of the internal surface areas of the vessels are stainless steel clad. The stainless steel cladding was not explicitly considered in the model, but accounted for in the density to capture the weight and with an effective composite thickness when considered in the strength calculations. The jacketing and insulation also were not explicitly modeled, but

the density of the shell was increased for the affected areas to account for the weight of the jacketing and insulation.

The material was assumed ideally elastic, perfectly plastic with the yield stress set at the material design stress intensity at 300ºF. A bi-linear elastic-plastic stress strain curve was used with a maximum 5% overstress. The FEA processing was done using the ABAQUS general purpose finite element analysis software running on an HP workstation with a UNIX based operating system.

In some cases, when the analysis had progressed sufficiently, the analyst chose to terminate the execution when it was apparent that the solution had been found. In this problem, many of the runs showed that the structure had failed and that the final solution was not going to change even though the software was capable of solving smaller and smaller increments.

The first step was the imposition of gravity including the hydrostatic pressure due to the contents. The second step was the pressure step. A target pressure of 2000 psi was set and internal pressure was ramped up until the load reached a level that would no longer give a valid solution or the analyst stopped the run because a sufficient number of iterations had been completed.

The results of interest were found by monitoring the displacement of the nodes that describe the location of the various nozzles. The displacements from the original, unloaded, locations were plotted for each increment of load.

The bottom head was nearly semi-elliptical at 191 psi. **Figure 6** shows a pronounced bulge at 194 psi. At 198 psi, the semi-elliptical head collapsed fully.

Figure 7 and **Fig. 8** show the displacements of the nozzles when the calculations were done considering both the carbon steel and the stainless steel liner as contributing to the structural strength. The very large displacements for small additional pressure load indicate structural collapse.

The results of the calculations only have meaning when they were compared to recognized standards. In the assessment of the results for the design loads, the pressures achieved in the limit load analysis were directly compared to the pressure rating requirements.

A summary of the results is given in **Table 2**. The analyst determined the limit load pressure as the largest load calculated then rounded down. This corresponds to the inflection point in the displacement curves seen in **Fig. 8**.

Table 2: Results of Limit Load Analyses

Configuration	Limit Load Pressure (psi)
Vessel, Carbon Steel Only	190
Vessel, Carbon Steel + Stainless Steel	210

The limit load calculated was adjusted to address two separate factors. The first adjustment was to convert the calculation that was done using a VonMises (octahedral stress), limit or yield surface to a Tresca (maximum shear stress), limit or yield surface. In this calculation, the factor of 1/1.15 was used. The second adjustment was the Code design factor of 2/3. The total adjustment was 0.58 times the limit load and the final pressure was rounded down.

The calculations performed in this study remove many of the overly-conservative assumptions concerning structural behavior inherent in classical calculations and give more detailed view of the expected performance of these pressure vessels. This work was not intended as a re-rating but as a measure of the expected structural strength using advanced techniques and recognized assessment methods.

Subsea Electronic Housing

A manufacturer of electronic equipment for subsea applications needed to optimize a design to achieve maximum water depths. Using a conceptual design, several analyses were performed using limit load methods. The primary design considerations involved geometric requirements associated with battery sizes and a design depth of 3,000 meters (9,840 feet). Initial efforts to size the dimensions of the design involved the use of a finite element model with shell elements. Once the geometry for the design was finalized, a limit analysis was performed using a model with solid eight-node hexagonal elements. The final analysis results demonstrated that the final geometry was adequately designed for the 3,000 meter depth requirement. Additionally, full-scale testing involving an external pressure of 10,000 psi proved the adequacy of the design. The sections that follow provided details on the analysis methods and results.

Preliminary Shell Model

Initial work involved using classical mechanics equations for basic sizing purposes. Once overall dimensions were provided, a preliminary finite element model using shell elements was constructed. In a design process, the shell element has an advantage in that its local thickness can be modified as an input variable, whereas solid elements require a complete reconstruction of the model geometry whenever dimensions such as wall thicknesses are changed. **Figure 9** provides a view of the basic shell finite element model.

Using the shell element model, wall thicknesses were determined for specific regions of the subsea housing that could meet both the geometric and operating requirements of the design criteria. The results of this portion of the analysis determined the geometry for the final design. Final use of the finite element method involved the construction of a solid model that included the main body of the housing, the lid, simulated bolting, and contact interaction between the lid and body.

Both the shell and solid models used limit load analysis. Elastic perfectly-plastic material properties for the aluminum 7075 material were input into the finite element model and external pressure was ramped up until convergence of the model was no longer possible. Because the primary intent of this project was development of a final design, the sections that follow provide specific details on the methods and results associated with the analysis of the solid element model.

Solid Model Analysis

The analysis of the three-dimensional finite element model using solid elements involved the following details:.

- Geometry included the outer cylinder of the main body housing, internal ribs oriented radially outward, 0.85-inch thick internal plate, and a 0.90-inch thick lid.
- Contact was modeled between the lid and the main body housing. Contact was generated on top of the ribs and in the recessed portion on each end of the housing.

- Bolting to attach the lid to the housing was accomplished by connecting nodes on the lid and body. This connection method was invoked at eight (8) regions on the housing located 45 degrees apart circumferentially.
- A symmetry plane was invoked half-way between the ends of the housing. This cut the 0.85-inch internal plate in half. As with the shell model, this boundary condition prevents nodes on the symmetry plane from displacing in the 3-direction and prevents rotations about the 1-direction and 2-direction.
- External pressure was applied to all outside surfaces of the housing including the lid and the cylinder. An external pressure of 10,000 psi was applied to the model. This value that exceeds that design requirement of 3,000 meters (approximately 4,370 psi), but was deemed high enough that convergence would be unlikely for the current design.

As with the shell models, the lower bound limit load was obtained by increasing external pressure on the finite element model to the point where the structure fails to withstand any additional load (i.e. convergence of the finite element solution was no longer possible). **Figure 10** provides an isometric view of the solid finite element model that includes details on the boundary conditions.

When ABAQUS solves a finite element problem, it produces a status file (e.g. *model_input.sta*) that reports the convergence parameters for the respective model. When performing a limit analysis, information contained within this file is useful. Provided in **Fig. 11** is the output data obtained for the solid finite element model. In this figure two columns are important.

- The data plotted in **RED** constitute an increment fraction of applied load. A value of 0.10 implies that 10 percent of the total load has been applied. The model stopped when an increment fraction of 0.941 was reached. For the problem at hand this means that the lower bound limit load is 94.1 percent of the total applied load (i.e. 10,000 psi). Consequently, the calculated lower bound limit load is 9,410 psi that corresponds to a subsea depth of 6,461 psi. To this value a design safety factor is applied.
- The data plotted in **BLUE** constitute deflection of a tied node where a bolt was assumed to exist. Although not necessarily applicable for the problem at hand, deflection data is often useful for creating load-deflection plots. At the end of the load step, disproportionately large deflections of the structure take place with small increases in load.

Having calculated the lower bound limit load, it is appropriate to discuss the design criterion that determined the allowable safe operating depth for the subsea housing. The calculated lower bound limit load is 9,410 psi (as shown in **Fig. 11)**, or 6,461 meters. Division 3 of the ASME Boiler & Pressure Vessel Code permits a factor of 2.0 on the lower bound limit load without restrictions. Using this design factor, a design pressure of 4,704 psi is calculated that corresponds to a sea depth of 3,230 meters. This design depth value exceeds the minimum design requirement of 3,000 meters. This design pressure is conservative and thought to satisfy the prescribed design requirements for the subsea housing, which was validated by experimental work that demonstrated the design was good for more than 7,000 psi. The only observed anomaly after testing was deformation of the internal ribs resulted in a plastic compressive deformation of 0.025 inches. There was no plastic deformation of the lid covering.

Figure 12 shows the deformation of the main body of the subsea housing from the finite element analysis with an external pressure of 9,410 psi. Note in this figure the deformation of the internal rib structure, which is consistent with the conditions observed experimentally in the external pressure testing.

Subsea Dented Pipeline

A subsea pipeline in the Gulf of Mexico was impacted by a ship anchor. This impact resulted in generating a longitudinally-oriented dent in the pipeline. Inspections revealed that no cracks were presented; however, concerns existed about the effects of the dent on the mechanical integrity of the pipeline. The line was fabricated from Grade X70 pipe having a diameter of 8.625 inches and a wall thickness of 0.656 inches. The dent had an estimated profile of 0.72 inches deep with a length of 13.8 inches based upon measurements scaled from photos taken subsea. The pipeline operates at a maximum allowable operating pressure (MAOP) of 7,700 psia and is located at a water depth of 7,150 feet.

Due to the thick wall of the pipe, solid three-dimensional elements were required. ABAQUS was used to process and post-process the analysis results. Elastic-plastic material properties along with nonlinear options for geometric displacements were used.

Finite element modeling was employed to assess the effects of the dent on the structural integrity of the pipeline. While some portion of this effort involved fatigue assessment due to cyclic pressures, the focus of the data for this paper is collapse due to external pressure. In deepwater applications, considerations require that external pressure be considered as a design load. In most subsea pipeline applications, the potential for collapse due to external pressure governs design, especially with regards to the required wall thickness. When deepwater subsea pipelines are permanently damaged in a manner than changes the ovality of the pipe, evaluation is required to determine the effect on the buckling capacity of the pipeline. The finite element analysis involved the following load steps.

- Step #1: Apply internal pressure to the inside of the pipe (4,525 psi - difference between MAOP and external pressure of 3,175 psi corresponding to 7,150 feet of sea water)
- Step #2: Move indenter to make contact with pipe
- Step #3: Push indenter into pipe to a depth of 1.0 inches
- Step #4: Remove indenter and determine residual dent depth (found to be 0.786 inches)
- Step #5: Remove internal pressure
- Step #6: Apply an internal pressure of 4,525 psi
- Step #7: Remove internal pressure (0 psi differential between inside and outside of pipe)
- Step #8: Apply external pressure of 12,700 psi to outside of sample (perform a limit analysis to determine buckling capacity of flowline considering the presence of a dent)

Steps #6 and #7 represent the extremes of a full pressure cycle. Stresses extracted from these load steps were used to calculate the stress range used in the fatigue analysis. Using the fatigue methods outlined in Appendix 5 of the ASME Boiler & Pressure Vessel Code, Section VIII, Divisions 2, the design fatigue life was calculated to be 76,012 design cycles. Assuming that the cyclic pressure condition spanning MAOP is typical,

there is no reason to expect that a fatigue failure will occur within the life of the flowline. This statement is based on the fact that no cracks are present and that the anchor dent represents a blunt defect without any appreciable metal loss.

Figure 13 shows details of the analysis model including the geometry of the indenter and the boundary conditions applied to the finite element model. To achieve the maximum depth of 1.0 inches in the half-symmetry model, an indenter force of 209,770 lbs. was required. Once the indenter was removed, a residual dent depth of 0.786 inches remained in the pipe. A total force of 419,540 lbs. was required to generate the dent.

Figure 14 shows the residual von Mises stress state that is calculated after the removal of internal pressure (corresponds to Step # 7). As noted in this figure, the stress field in the vicinity of the dent exceeds the material yield strength of 70 ksi. This trend is also observed 90 degrees relative to the location of the dent on the side of the pipe. It is these latter stresses that are of primary concern when discussing the capacity of the pipeline to resist buckling due to external pressure.

In addition to addressing the effects of cyclic internal pressure on the fatigue life of the flowline, SES also performed a limit analysis to determine the impact of the dent on the buckling capacity of the pipe. **Figure 15** shows the deflection of the dented pipe region as a function of external pressure. A limit analysis involves the application of increasing loads (in this case external pressure) to the point where disproportionate displacements occur. The load at which this occurs is defined as the lower bound collapse load. As shown in **Fig. 15**, once a pressure of approximately 14,000 psi is reached, the displacement increases without bound, defining this pressure as the lower bound collapse load. The external pressure at the 7,700-ft water depth (shown as the **SOLID RED** line in this figure) is approximately 25 percent of the 14,000 psi pressure value, indicating that a safety margin of 4 exists relative to the external pressure at which buckling is likely to occur. In other words, it is unlikely that the flowline will buckle even in the event of complete internal pressure loss at a water depth of 7,700 feet.

CONCLUSIONS

Analysis results for four unique engineering applications have been presented. Prior to advances made in the application of limit analysis using high speed computers, engineers were required to reduce complex structures into simplified geometries that would permit stability analysis using closed-form solutions. In the absence of more rigorous analysis methods such as those discussed in this paper, these simplifications were the only options that existed. The drawback to these approaches was that overly-conservative design criteria were required that resulted in the construction of heavy structures with unnecessarily high levels of stiffness. Along the same lines, limitations existed in terms of what engineers really understood regarding structural stability and the mechanisms that could lead to instability and catastrophic failure.

The method of limit analysis resolves many of the shortcomings associated with stability analysis based on classical methods. As shown in the four examples presented in this paper, limit analysis permits the evaluation of structural stability for complicated structures including material non-linearities and surface contact. The benefits are two-fold. First, \engineers are able to evaluate and design complex structures in conjunction with more traditional design approaches based on stress and deformation criteria. Secondly, when performing limit analyses engineers are better positioned to understand the potential failure mechanisms due to overload and are therefore able to establish design conditions to ensure the safe and reliable operation of the structure.

REFERENCES

[1] ASME, Boiler and Pressure Vessel Code, Section VIII, Division 1, Rules for Construction of Pressure Vessels; Section VIII, Division 2, Rules for Construction of Pressure Vessels, Alternative Rules; and Section II, Materials, Part D, Properties, The American Society of Mechanical Engineers, Three Park Avenue, New York, NY 10016.

[2] Kalnins, Arturs, WRC Bulletin 464, Guidelines for Sizing of Vessels by Limit Analysis, August 2001, Welding Research Council, Inc. Three Park Avenue, New York, NY, 10016.

[3] ASCE Standard 7, Minimum Design Loads for Buildings and Other Structures, American Society of Civil Engineers,1801 Alexander Bell Drive, Reston, Virginia 20191-4400.

[4] ABAQUS/Standard version 6.4, Hibbitt, Karlsson & Sorensen, Inc. 1080 Pawtucket, RI 02860-4847

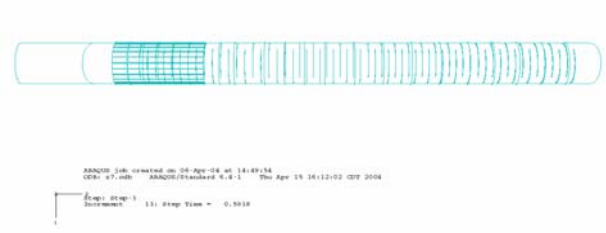

Fig. 1 - Finite Element Model, “Edges” of Features

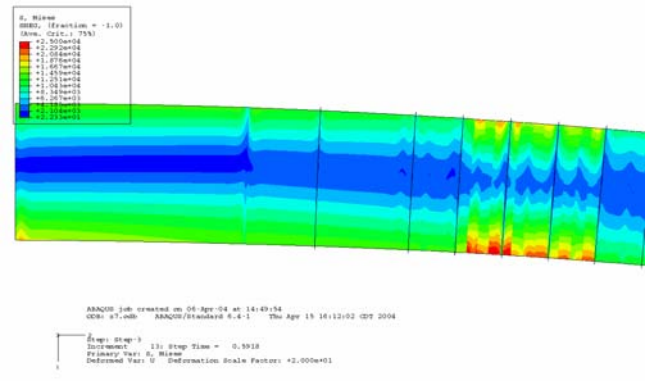

Fig. 2 - Tower VonMises Stress, Gravity + External Pressure, Wind Ramped to DM = 1.78 (Unreinforced) (Contour Mises stress range: 0.02 ksi to 25.0 ksi)

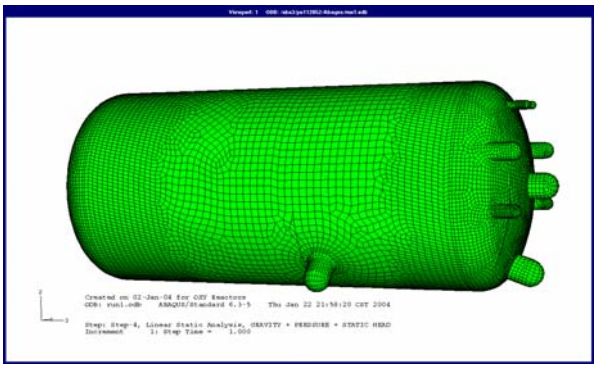

Fig. 5 - Finite Element Model, Pressure Boundary

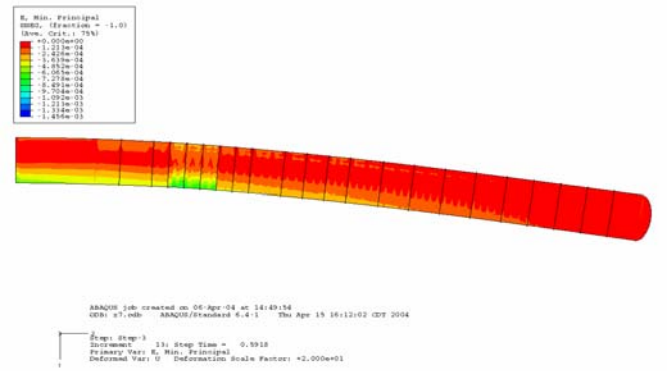

Fig. 3 - Displaced Shape, Minimum Principal Surface Stress, Gravity + External Pressure = Vacuum, Wind Ramped to DM = 1.78 (Unreinforced) (Contour strain range: 0.0 to -0.145%)

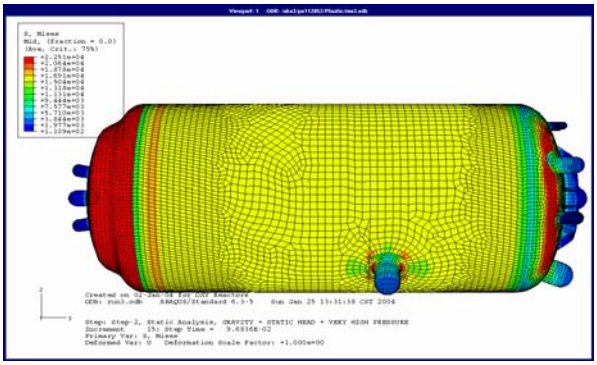

Fig. 6 - Limit Load Displacement, 194 psi (Contour Mises stress range: 0.11 ksi to 22.5 ksi)

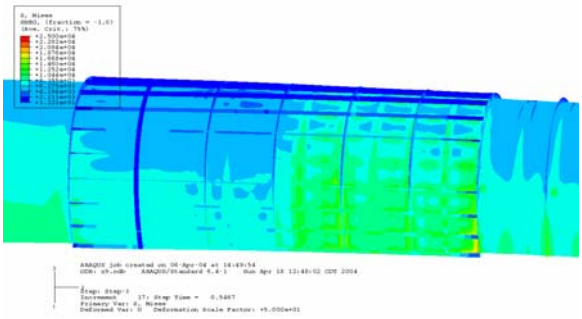

Fig. 4 - Tower VonMises Surface Stress, Gravity + Basic Wind Load, External Pressure Ramped to DM = 2.19 (Reinforced) (Contour range: 0.03 ksi to 25.0 ksi)

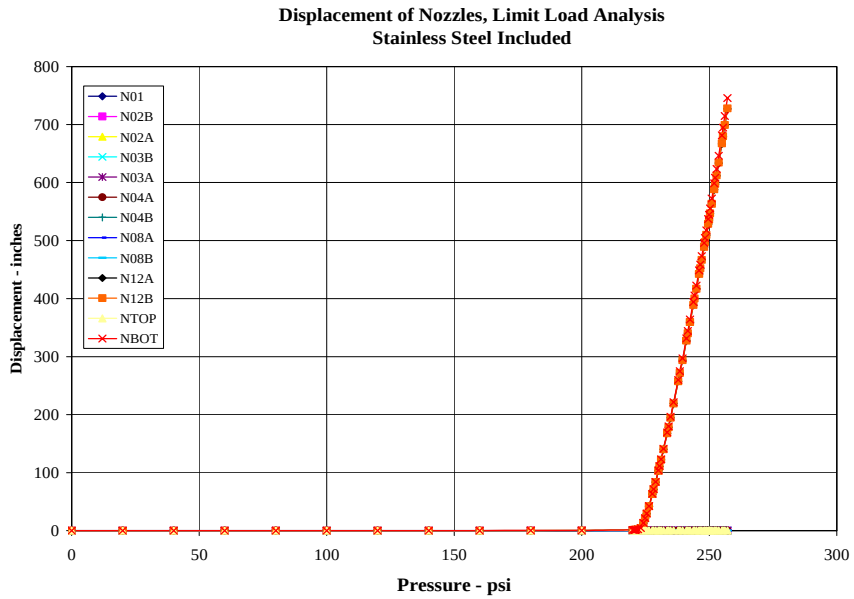

Fig. 7 - Results of Limit Load Analysis, Stainless Steel Included

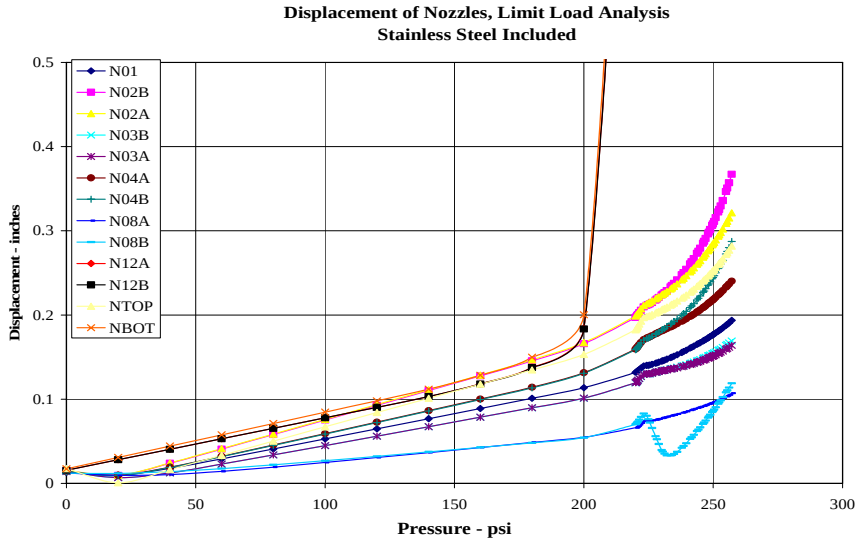

Fig. 8 - Detail of low-level displacement data presented Figure 7

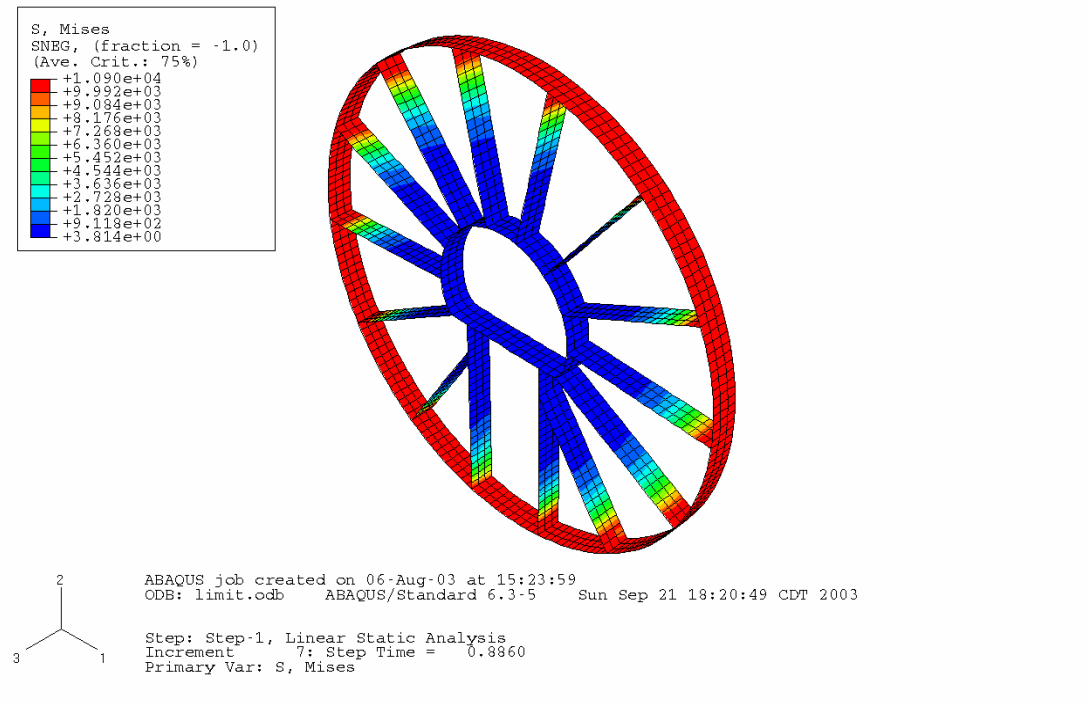

Fig. 9 - Von Mises stress contour plot for finite element model

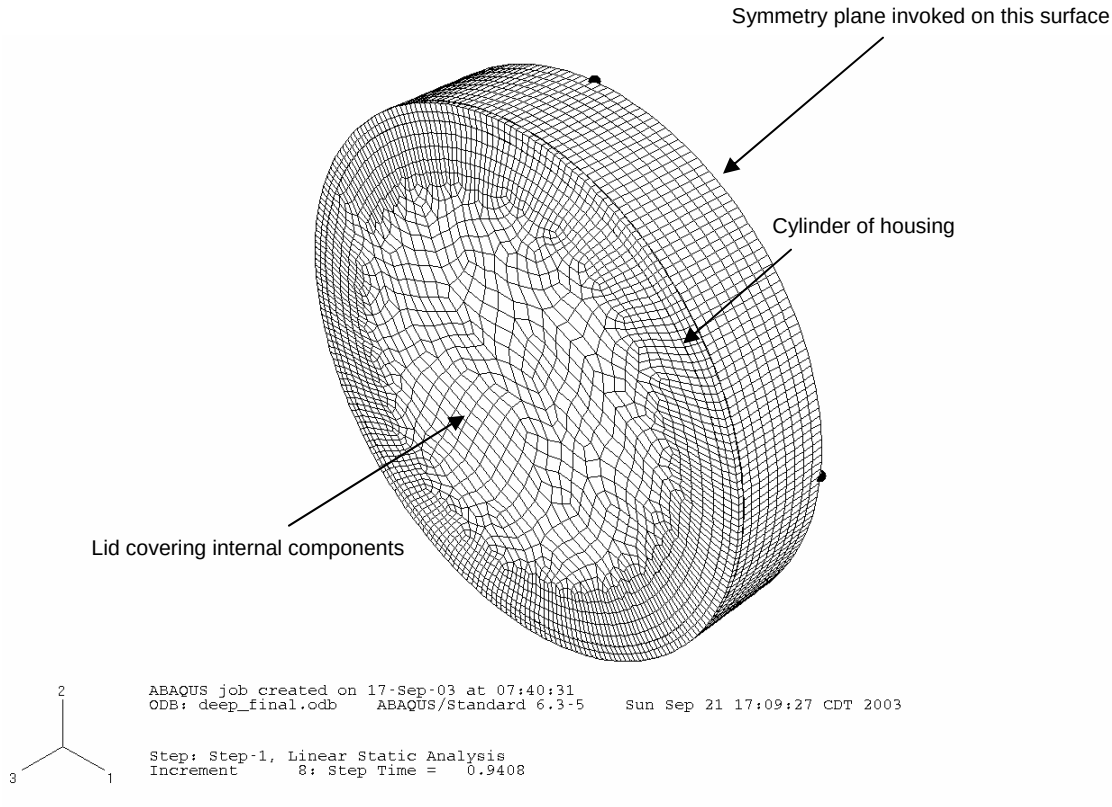

Fig. 10 - Isometric view of solid finite element model

```
ABAQUS VERSION 6.3-5                                DATE 21-SEP-2003  TIME 17:09:37
 SUMMARY OF JOB INFORMATION:
 MONITOR NODE:   25752  DOF:  2
 STEP  INC ATT TOTAL  TOTAL      STEP       INC OF       DOF
               ITERS  TIME/    TIME/LPF    TIME/LPF    MONITOR
                      FREQ

   1     1   1    6  0.100      0.100       0.1000     -0.00267
   1     2   1    5  0.200      0.200       0.1000     -0.00481
   1     3   1    5  0.350      0.350       0.1500     -0.00782
   1     4   1    5  0.575      0.575       0.2250     -0.0124
   1     5   1   11  0.913      0.913       0.3375     -0.0241
   1     6   2    6  0.934      0.934       0.02187    -0.0359
   1     7   2    5  0.940      0.940       0.005469   -0.0469
   1     8   3    4  0.941      0.941       0.001000   -0.0574

 THE ANALYSIS HAS NOT BEEN COMPLETED
```

Fig. 11 - ABAQUS status file output for finite element model

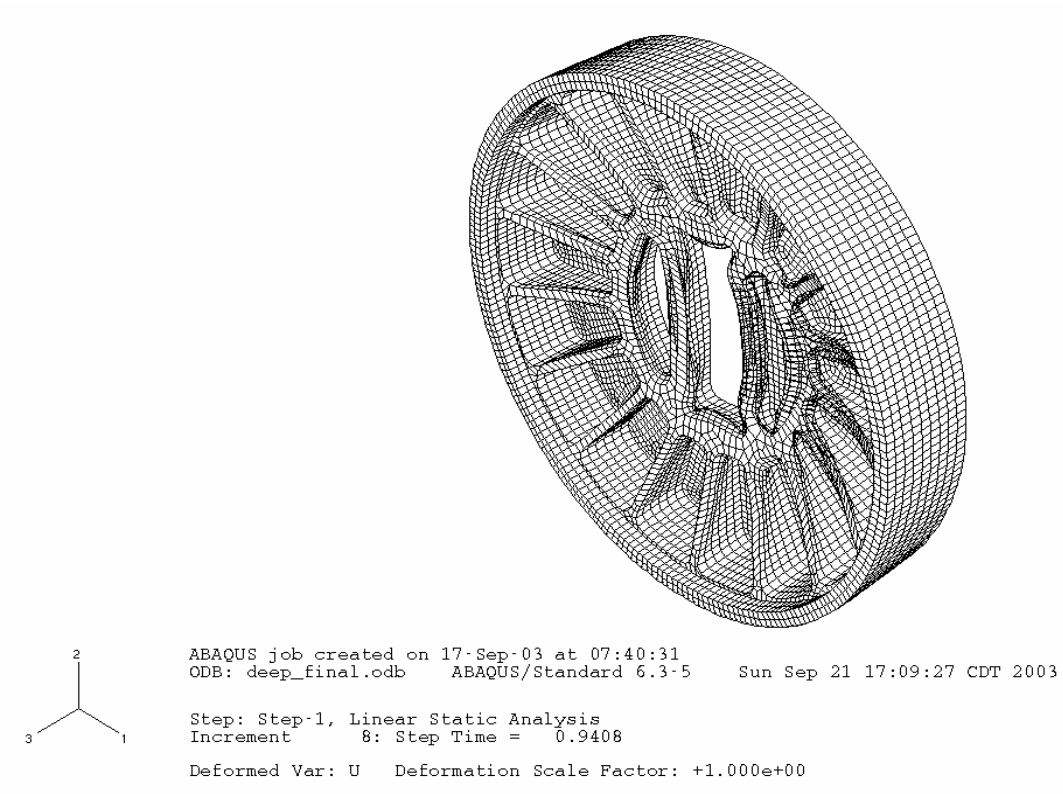

Fig. 12 - Displaced shape for the solid finite element model (1X magnification)

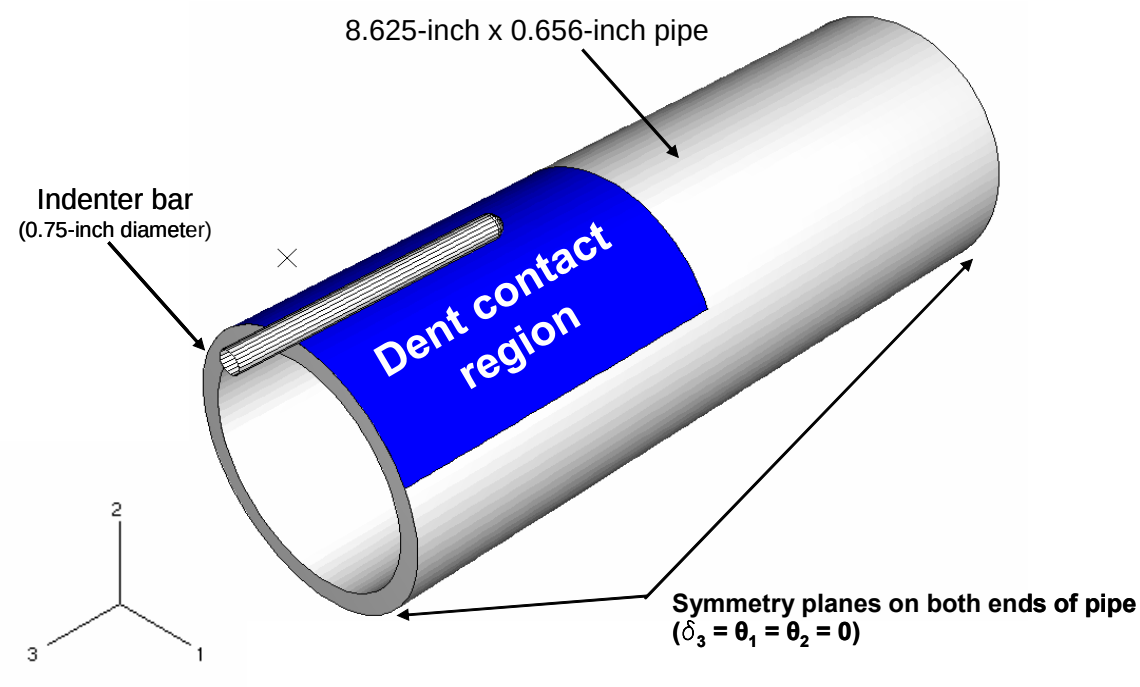

Fig. 13 - Geometry for finite element model (half-symmetry geometry)

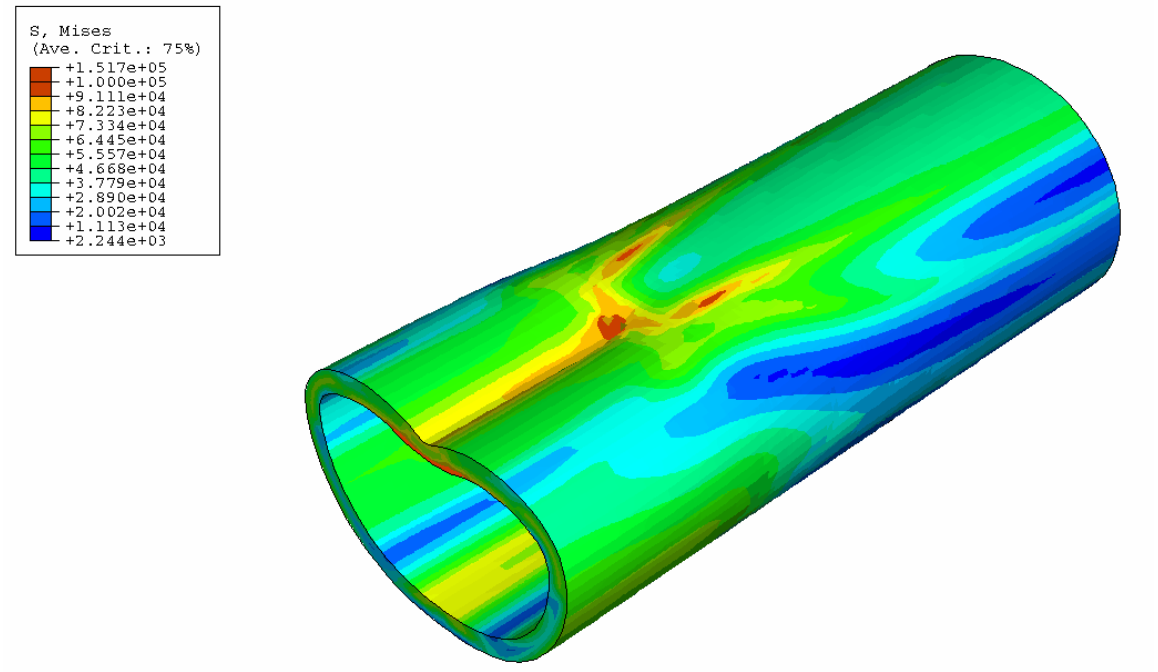

Fig. 14 - Von Mises stress after internal pressure removed (residual stress state)
(Magnification factor on displacement of 2.4)

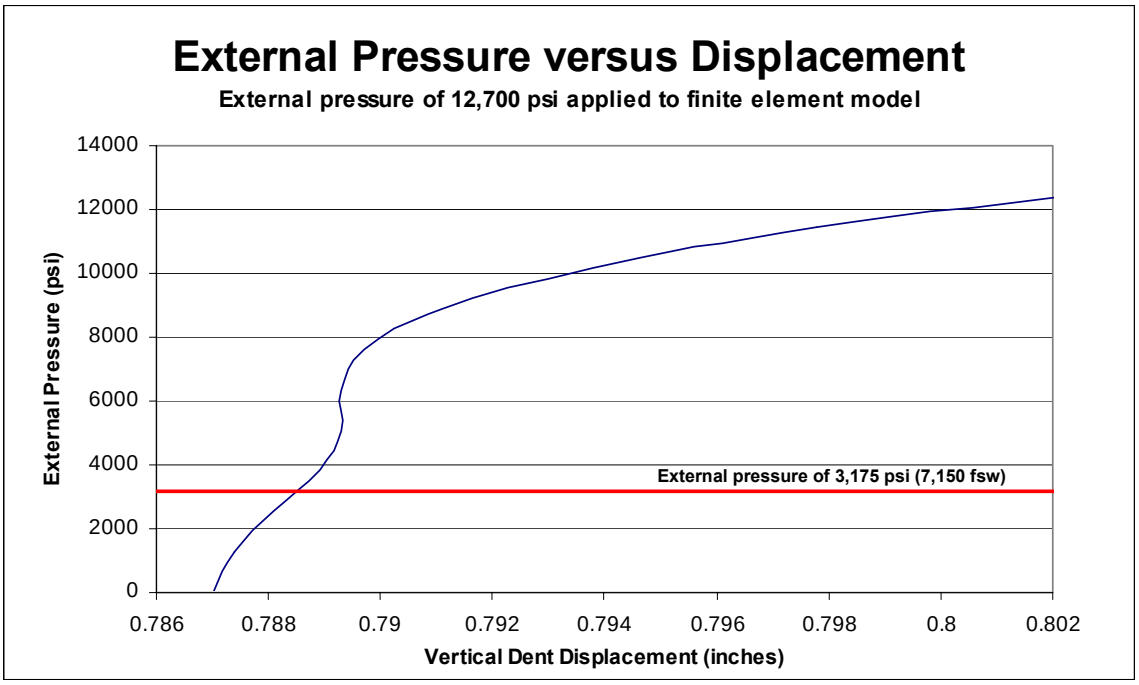

Fig. 15 - Response of dented pipe to elevated external pressures